Proc. of JSCE,
No. 161, 1969-1

EXPERIMENTAL STUDY ON THE PROPAGATION OF STRESS WAVE IN COHESIVE SOILS*

*By Koichi Akai**, Mineo Tokuda*** and Tsutomu Kiuchi*****

1. Introduction

Generally speaking, in proceeding the investigation on the aseismatic design of structures there exist two ways of approach, one is the way using the theory of vibration and the other is that based on the theory of wave propagation. The former which treats the object as a whole mass is efficient to know and analyze the response behavior of the mass, and the latter is suitable for analyzing phenomena generating at any point in the material.

In studying the one-dimensional stress wave propagation in soils, the theoretical work by Salvadori *et al*[1] would be adaptable. Two types of inelastic materials postulated are a locking medium and a dissipative medium. For the former it was indicated that a pressure pulse might generate either a supersonic shock wave, or a subsonic wave with an elastic precursor, or a purely elastic wave. For the latter, on the other hand, the time history of stress and strain under a pressure pulse was given and it was shown that eventually the medium would reach an unstressed state and remain at rest but with parmanent displacements.

The attenuation of plane stress waves generated by a decaying surface pressure in a bi-linear medium was investigated by Skalak and Weidlinger[2], to obtain an approximate solution to the problem of a medium with a stress-strain diagram of positive curvature. One-dimensional wave equations were derived, and it was demonstrated that, beyond a given distance from the surface, the intensity of the peak stress and particle velocity depended only upon a single parameter.

Further, Weidlinger and Matthews[3] investigated the shock and reflection in a nonlinear medium, considering the characteristic of porous or granular solids. It was shown that the propagation velocity of the shock wave depended on the secant modulus and, therefore, it was a function of both the intensity of the applied pressure and the degree of nonlinearity of the stress-strain curve.

Heierli[4] performed both theoretical and experimental studies on the problems of one-dimensional waves in inelastic media such as soils. The fundamental problem involved the prediction of the stresses and particle velocities as functions of time and depth in a soil column when the pressure at the surface is known. In order to solve this problem, experiments were conducted to determine the dynamic stress-strain curve of the material. These wave propagation experiments were shown in which the wave phenomena were observed and compared with the theoretical values.

One-dimensional wave propagation in soils as a visco-elastic compacting medium was throughly treated by Seaman[5]. In this research soil behavior during stress propagation was studied on a sand and two kinds of clay by making one-dimensional wave propagation tests on 5-meter long columns of the soils. Attempts were made to predict this behavior by determining soil properties in dynamic compression tests on small samples and by using these properties in a variety of mathematical models for soil.

The present investigation concerns with behaviors of the pressure wave attenuation through cohesive soils. Since Japan lies on one of the notorious seismic bands in the world, we have to establish a comprehensive aseismatic design method, taking the behaviors of ground and the interaction problems between structure foundations such as footings or piles and ground into consideration. From this point of view wave characteristics at the interface of two different materials are also investigated in this experimental study.

In this study the authors are so interested in the behavior of ground excited by the earthquake motion and wish to know what phenomena will occur at any point in the ground during the earthquake disturbance, that the analyzing method by the wave propagation theory will be used mainly in proceed-

* Presented at the 23rd Annual Meeting of J.S.C.E., Oct., 1968.

** Dr. Eng., Professor of Civil Engineering, Kyoto University.
*** M.S.C.E., Official, Port and Harbour Bureau, Ministry of Transportation.
**** Graduate course student, Kyoto University.

ing the study. We regard the earthquake motion as a pulsative disturbance which acts in very short time rather than as a periodic dynamic one which continues for fairly long time, and then clarify the characteristics of the stress wave propagating through soil when it is excited by such a shock disturbance.

Owing to the experimental apparatus only the longitudinal or dilatational wave is dealt with in this study, though we should not forget that the shear or distortional wave plays an important role in real earthquakes. In performing the theoretical analysis many adequate assumptions are used in order to make the mathematical treatment possible, and they are explained in detail when they appear.

2. Experiments

(1) Soil specimen and experimental apparatus

Specimen was made as the manner that, after mixing the dry powder of clay obtained at the southern part of Kyoto city with sufficient amount of water, it was consolidated in a large scale soil box so as to have an adequate water content. Some physical properties of the specimen used are summarized in Table 1. After filling the box with the remoulded clay a bag made of strong vinyl sheet was mounted on the clay stratum and the hydrostatic pressure was acted on it through the vinyl bag. The pressure used for consolidating the clay was 0.5～0.6 kg/cm² and water was drained from the two sand layers which sandwiched the clay stratum.

Table 1 Physical properties of clay specimen.

Specific gravity	2.60
Particle composition	
Clay fraction (<5 μ)	12.5%
Silt fraction	71.0%
Sand fraction	16.5%
Liquid limit	51.5%
Plasticity index	31.8%

Consolidation was completed usually in about 20 days and the ultimate water content was approximately 40～43%, the unconfined compression strength of the specimen obtained being about 0.13 kg/cm².

After the consolidation was over the side plate of the soil box was taken off and a cylindrical tube made of tin-plate was pushed into the clay stratum from this side, and thus the specimen was obtained. The specimen which was compressed to some extent during sampling had a cylindrical form with 6 cm in diameter and about 60 cm in length after sampling.

The outline of the experimental apparatus for impact test is shown in Fig. 1 and the general scheme of this test is seen in Photo. 1. The clay specimen (S) was sustained horizontally by some ribbons made of cloth attached to the rigid frame (F). One end of the specimen was connected with some kinds of reaction material (R) of which rigidity was different from the soil specimen. The other end of the specimen was the impact end (I) where a rigid steel plate was attached in order to obtain the uniform distribution of the impact force to it, and a small accelerometer (a) was mounted on the steel plate to measure the input force to the specimen by the impact.

(W) in Fig. 1 is a weight hanged down from the frame, and it struck the impact end of the specimen to generate the pulsative force. At each point of the specimen a very small pressure gauge (P) was embedded to measure the pressure propagating

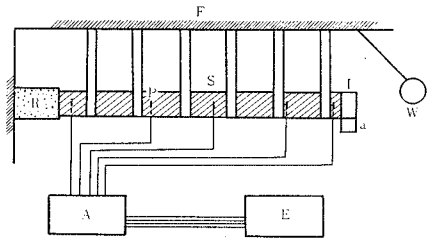

a : Accelerometer
A : Amplifier
E : Electro-magnetic oscilloscope
F : Frame
I : Impact plate
P : Pressure gauge
R : Reaction material
S : Specimen
W : Weight

Fig. 1 Experimental apparatus for impact test.

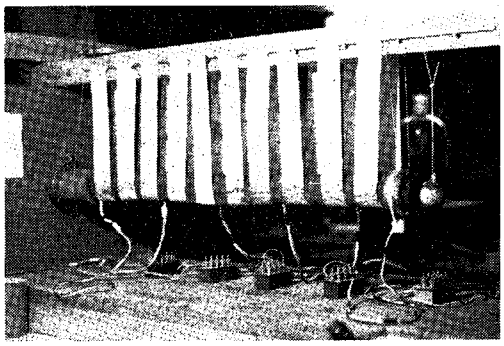

Photo. 1 Impact test apparatus.

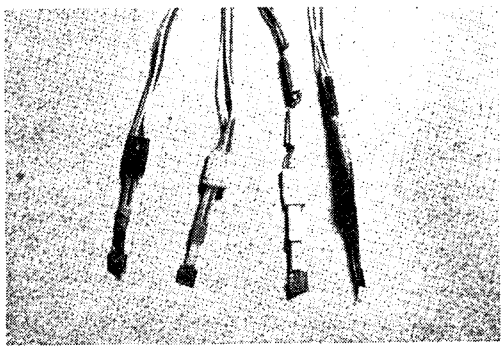

Photo. 2 Pressure gauges.

through the specimen. The gauge was 6 mm in diameter and 0.5 mm in thickness (Photo. 2) and was stuck on a small brass plate. It had the maximum measuring capacity of 2 kg/cm².

Pressures propagating through the specimen by the impact were picked up by the pressure gauges embedded in the soil specimen, and the electrical signal from gauges was amplified by the amplifier (A) and recorded continuously by the electro-magnetic oscilloscope (E).

(2) Experimental procedure

In the impact test the propagating stress was measured at five points by the pressure gauge and each measuring point had intervals of about 15 cm. Two of these measuring points were placed so near the impact end and the reaction end that they could measure the stress wave given at the impact end and that generated in the vicinity of the reaction end, respectively.

The reaction end (R) in Fig. 1 was changed with some kinds of material which had different rigidities relative to the soil specimen. This was for the purpose of investigating the state of the interaction between the incident wave and the reflected one owing to the relative rigidity of the reaction end and the soil. Materials of the reaction end used were steel, cement mortar, dense sand, loose sand, very soft clay and rubber foam, and their characteristic impedances ρc are summarized in Table 2 (ρ: density, c: celerity).

Table 2 Characteristic impedance for each reaction end.

Materials	ρ(g/cm³)	c(cm/sec)	ρc(g/cm²·sec)
Clay specimen	1.98	70×10^2	13.9×10^3
Steel plate	7.80	5260	4100
Cement mortar	2.07	3230	670
Dense sand	1.95	484	82.3
Loose sand	1.25	183	23.0
Soft clay	1.65	10	1.7
Rubber foam	0.029	?	≃0

The weight (W) in Fig. 1 lifted up to an adequate height was dropped down like a pendulum and struck the impact end (I) to generate the impact force there. The electro-magnetic oscilloscope was switched on to send the recording paper continuously just when the weight was released, and it recorded the stress wave form picked up by the pressure gauges at each point. The same experiments were carried on changing the reaction end with six kinds of material mentioned above.

A typical record obtained in this experiment for the steel end is shown in Fig. 2, and the calibrating procedure for the pressure is illustrated in the same figure. Provided this record is drawn as modelling in the plane which has the coordinates of distance,

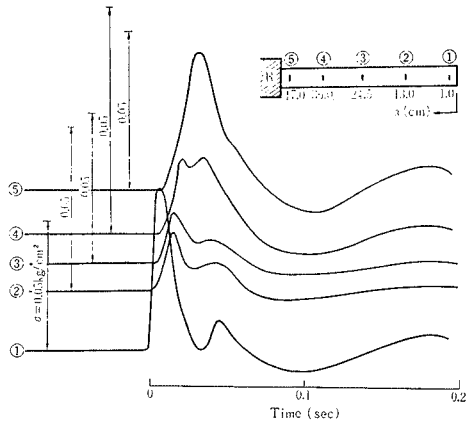

Fig. 2 Typical test result (steel end).

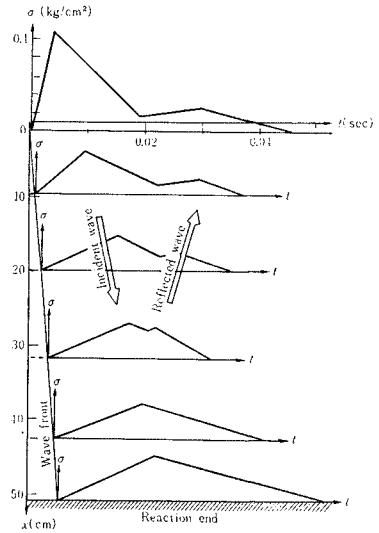

Fig. 3 Typical pressure wave at each point in clay column.

time and pressure, $x-t-\sigma$ plane, it can be shown as Fig. 3.

From this figure we can find following characteristics about the propagating pressure wave;

1) The peak pressure attenuates with distance.
2) The time required to reach its peak pressure, often called as "the rise time", increases with distance.
3) The time for the pressure to attenuate to a certain extent of its peak value, "the decay time", increases with distance.
4) The reflected pressure wave advancing adversely from the reaction end is recorded clearly by some pressure gauges at a fair distance from the reaction end.
5) Near the reaction end the incident wave and the reflected wave are superposed on each other and the resultant wave form is similar to a hill with only one peak, and we can find

that there exists a higher pressure than at other middle points.

3. Analysis of Propagating Stress

(1) Attenuation of stress wave

In the explanation of Fig. 3 it has been described that the pressure (or the peak pressure) attenuated with distance. In the real earthquake motion the seismic wave attenuates when it propagates through the ground, and the following three reasons might be regarded as the causes of this wave attenuation[6];

1) Energy dissipation into the space as the seismic wave propagates through the ground.

2) Reflection, refraction or penetration of the wave at the interface of different materials.

3) Energy absorption by the medium.

In this study the authors deal with a plane wave, or one-dimensional wave, which propagates through a soil column. Consider a column of clay with a density ρ, and it is briefly assumed that the deformation cannot be recovered under the load decreasing.

The semi-logarithmic plot of the pressure given to the impact end to the time in the experiment is illustrated in Fig. 4. From this figure we can find that there exists an exponential relationship between the applied pressure and the time. The applied surface pressure, $p(0, t)$, is given by the following form;

$$p(0, t)=p_0 e^{-\theta t} \quad \cdots\cdots(1)$$

in which p_0 denotes the peak intensity of the applied surface pressure and θ the attenuation constant.

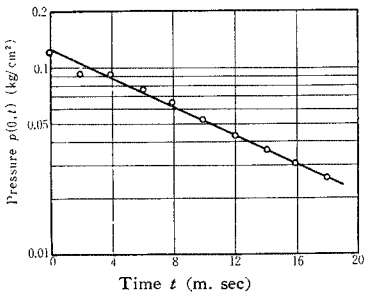

Fig. 4 Applied surface pressure, p (0, t), for impact test.

Fig. 5 illustrates the state of the compressive pressure wave propagating one-dimensionally through the column with density ρ. At the time t the wave front reaches the distance x from its origin and the impact end moves in the distance u, and at the time $t+dt$ the wave front and the impact end reach the distance $x+dx$ and $u+du$, respectively.

Fig. 6 shows the applied surface pressure, $p(0, t)$, which reaches its peak intensity, p_0, at the instance of impact and then decays exponentially with time.

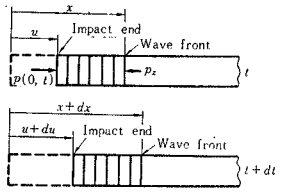

Fig. 5 Propagation of longitudinal wave.

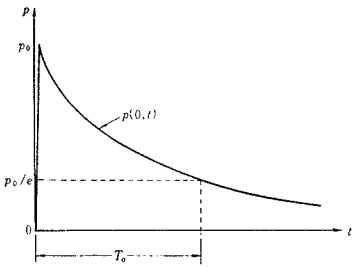

Fig. 6 Applied surface pressure, $p(0, t)$, *vs.* time.

Because of the pressure form shown in this figure, the pressure, p_x, at the wave front of distance x in Fig. 5 is found to be the peak pressure at that place.

By the assumption that the deformation is irrecoverable, the particle velocity behind the wave front is equal to $\dot{u}$ everywhere and, therefore, the momentum at the time t is equal to $\rho \dot{u} x$ and that at the time $t+dt$ is $\rho \dot{u}(x+dx)$. Then the following equation of movement is obtained;

$$\frac{\rho \dot{u}(x+dx)-\rho \dot{u} x}{dt}=p_x$$

then,

$$p_x=\rho \dot{u} \frac{dx}{dt} \quad \cdots\cdots(2)$$

in which p_x is the pressure at the wave front with distance x and, at the same time, the peak intensity at that place as described above.

dx/dt defines the propagation velocity of the wave front, and if the stress-strain relationship is assumed to be linear under the stress increasing, the velocity of the wave front, dx/dt, is constant.

Defining t as the time which the wave front takes in travelling the distance x, on the other hand, the following equation is derived from the law of conservation of momentum;

$$\rho \dot{u} x=\int_0^t p(0, t)dt \quad \cdots\cdots(3)$$

where $p(0, t)$ is the applied surface pressure and is defined by Eq. (1).

From Eqs. (2) and (3) the peak pressure, p_x, at each place is related to the distance, x, by

$$p_x=\frac{1}{x}\frac{dx}{dt}\int_0^t p(0, t)dt \quad \cdots\cdots(4)$$

Substituting Eq. (1) into Eq. (4) and integrating it, we get

$$p_x=\frac{p_0}{\theta}\frac{1}{x}\frac{dx}{dt}(1-e^{-\theta t}) \quad \cdots\cdots(5)$$

In order to get the nondimensional form of the peak pressure, p_x, and the distance, x, the former is divided by the peak intensity of the applied surface pressure p_0, and the latter by c_0T_0, in which c_0 is the propagation velocity of the wave front and T_0 the decay time of the surface pressure[7] (see **3.** (**3**)).

For the relationship between the dimensionless peak pressure p_x/p_0 and the dimensionless distance x/c_0T_0, the evaluated result from Eq. (5) is shown in Fig. 7 with solid line. The conditions used in this evaluation are as follows; for the applied surface pressure in Eq. (1), the expression $p(0, t)=p_0e^{-47t}$ (t in sec) is given from sequence of Fig. 4. Thus for the propagation velocity of the wave front, $dx/dt=c_0=$ 70 m/sec, and for the decay time of the applied pressure, $T_0=0.005$ sec. All these values are those measured in the experiment.

The experimental results of the dimensionless peak pressure, p_x/p_0, versus the dimensionless distance, x/c_0T_0, are plotted in Fig. 7. When we compare the measured value with the calculated one from Eq. (5) in Fig. 7, it is clear that the measured peak pressure attenuates more rapidly with distance than the calculated one.

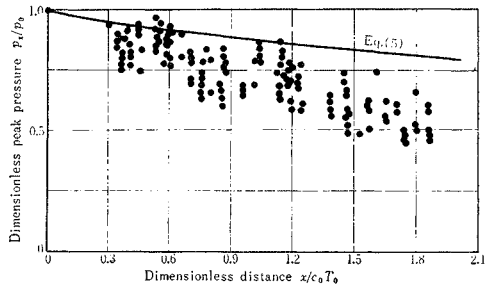

Fig. 7 Peak stress attenuation with distance.

As the causes of this discrepancy the followings are thought of;

1) In spite of the assumption of the one-dimensional wave propagation in the theory, it is not precisely in the experiment, for the lateral displacement is not confined there. Therefore, some energy of the propagating wave will be consumed into the lateral movement of the soil column in the experiment, and then the pressure may attenuate much more than the case in which it propagates one-dimensionally.

2) It is assumed that the peak pressure will generate at the wave front in the theory. In practice, however, the pressure reaches its peak intensity after a little behind the wave front as we have seen in Fig. 3. In these intervals some energy of the wave may also be considered to be consumed.

(2) Rise time of stress wave

As we have seen in Fig. 3, the time for the pressure wave to take in reaching its peak intensity increases with distance from the impact end. The time in which the pressure attains its peak intensity from the instance of the impact is often called as "the rise time". The cause of the increase in the rise time with distance might be considered as follows.

The wave front and the wave peak propagate with the velocities determined by the elastic moduli corresponding to those stress levels on the stress-strain relationship, respectively, and in usual those moduli are not always same. In the present case the modulus at the wave peak, E_p, is smaller than that at the wave front, E_0, as shown in Fig. 8. Therefore, the wave peak propagates with lower velocity than the wave front. This situation is illustrated in Fig. 9; here for convenience of analysis the velocities of the wave front and of the wave peak, c_0 and c_p, respectively, are assumed to be constant. As in Fig. 9, if the velocity of the wave front is higher than that of the wave peak, that is to say if $c_0>c_p$, the rise time, t_x, will be found to increase with distance.

Now we define the rise times of the applied surface pressure and the pressure at distance x as t_0 and t_x, and the velocities of the wave front and the wave peak as $c_0(=\sqrt{E_0/\rho})$ and $c_p(=\sqrt{E_p/\rho})$, respectively. From the geometrical relation in Fig. 9 we obtain the following nondimensional relationship;

$$\frac{t_x}{t_0}=1+\left(\frac{1}{c_p}-\frac{1}{c_0}\right)\frac{x}{t_0} \qquad \cdots\cdots(6)$$

From this equation we can get the rise time, t_x, at any distance, x, by using the values of velocities of the wave front and the wave peak.

The experimental data are divided into three gro-

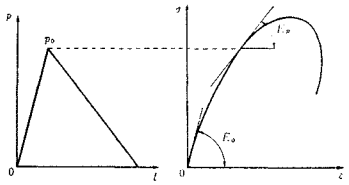

Fig. 8 Elastic moduli corresponding to the wave front and the peak stress.

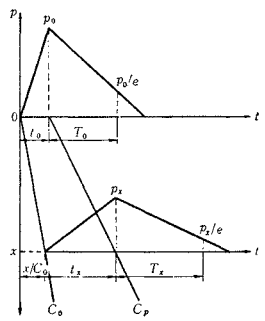

Fig. 9 Rise time and decay time at each point.

ups of the peak pressure intensities, p_0=0.05, 0.10 and 0.15 kg/cm^2. The conditions used in the calculation are as follows.

The dynamic stress-strain curve of saturated clay in the unconfined compression test is shown in Fig. 10. The elastic moduli corresponding to the above three stress levels and the propagation velocities of the wave front and the wave peak determined by those moduli are;

for the wave front : E_0=93 kg/cm^2, c_0=67.8 m/sec,
for the wave peak : $E_{0.05}$=77 kg/cm^2,
$c_{0.05}$=19.5 m/sec,
$E_{0.10}$=43 kg/cm^2,
$c_{0.10}$=14.5 m/sec,
$E_{0.15}$=30 kg/cm^2,
$c_{0.15}$=12.3 m/sec.

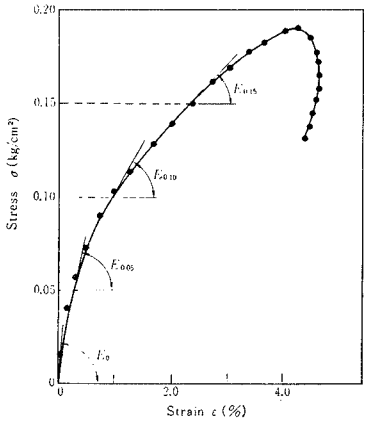

Fig. 10 Elastic moduli corresponding to three stress levels.

The calculated results using these conditions and the experimental data are compared in Fig. 11. In this fiigure we notice that the difference between the calculated results and the experimental data might be due to the assumption of constant velocity of the wave peak in deriving Eq. (6). In practice the peak pressure attenuates with distance and, in accordance with this decrease in the peak intensity, the propagation velocity, c_p, increases asymptotingly to that of the wave front, c_0, ultimately.

(3) Decay time and duration time of stress wave

The time in which the pressure waves takes in decreasing its intensity from the peak value, p_0, to that multiplied by $1/e$(=0.368) is often called as "the decay time" or "the attenuation time". As shown in Fig. 9, we define the decay times of the applied surface pressure and the wave at distance x as T_0 and T_x, respectively.

The total area enclosed by the pressure-time curve is called as "impulse" and is represented by $\int_0^t p(t)\cdot dt$. Under the normal level of the pressure this impulse at each depth is found to be constant[6], and considering this fact, we obtain the following equation by virtue of the geometrical relationship in Fig. 9;

$$\frac{T_x}{T_0}=\frac{t_x}{T_0}+\left(1+\frac{t_0}{T_0}\right)\frac{1}{\frac{p_x}{p_0}} \quad \cdots\cdots(7)$$

If we define the time for the pressure to take in decreasing its intensity to the peak pressure multiplied by $1/e$ from the instance of the impact as "the duration time of pressure wave", Eq. (7) is reduced using Eq. (4);

$$\frac{t_x+T_x}{t_0+T_0}=\frac{p_0}{p_x}=\frac{p_0 x}{\frac{dx}{dt}\int_0^t p(0,t)dt} \quad \cdots\cdots(8)$$

where dx/dt is the propagation velocity of the wave and $p(0, t)$ the applied surface pressure.

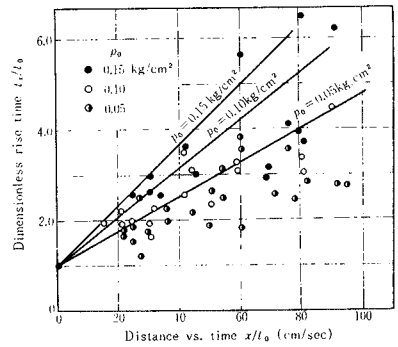

Fig. 11 Rise time increasing with distance.

For the duration time of the pressure wave, the comparison of the calculated result with the measured one is illustrated in Fig. 12. Both theoretically and experimentally the duration time increases with distance, and it may be found from Eq. (8) that the duration time enlarges for soft soil and for higher intensity of the peak pressure. As in Fig. 12 the experimental results have fairly larger values than the calculated ones.

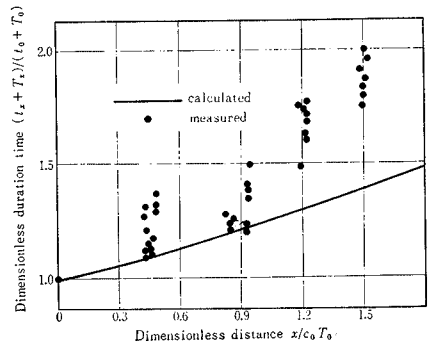

Fig. 12 Duration time increasing with distance.

4. Wave Characteristics at the Interface of Two Different Materials

(1) Reflection and refraction of wave

When the wave incidents to the interface of two different materials, some of the wave is reflected at the interface and the residual wave penetrates into the second material. These two phenomena are known as the reflection and the refraction of wave at the interface, respectively.

For example the seismic wave propagating through the ground will be reflected when it reaches the base of a structure, and the incident wave and the reflected one will interact with each other in the ground near the foundation of the structure; therefore the resultant wave would be different from that at another place.

In studying on the aseismicity of the foundation ground itself, this phenomenon cannot be neglected. On the other hand, this also should be known when we investigate the state of waves generated in each soil layer in the case of the seismic wave propagation through some layered ground.

Now let us consider the incidence of dilatational or longitudinal wave to the interface of two media which have the densities, ρ_a and ρ_b, and the state of reflection and refraction of this wave incidence is illustrated in Fig. 13[9]. At the interface there are now four separate boundary conditions; on both sides of the boundary the following four quantities must be equal.

1) the normal displacement $\Sigma u_a=\Sigma u_b$
2) the tangential displacement $\Sigma v_a=\Sigma v_b$
3) the normal stress $\Sigma \sigma_a=\Sigma \sigma_b$
4) the tangential stress $\Sigma \tau_a=\Sigma \tau_b$

.....(9)

Let the amplitude of the incident dilatational wave be A_1, those of the reflected and refracted dilatational wave be A_2 and A_4, and those of the corresponding distortional wave be A_3 and A_5, respectively (see Fig. 13). Substituting into the boundary conditions yields four correlations between the amplitude and it has been found that the boundary conditions are satisfied when assuming that Huygens' principle could be applied to these waves. This construction leads, as in the case of light, to the following relationship;

$$\frac{\sin\alpha_1}{c_1}=\frac{\sin\alpha_2}{c_1}=\frac{\sin\beta_2}{c_2}=\frac{\sin\alpha_3}{c_3}=\frac{\sin\beta_3}{c_4} \quad \cdots\cdots(10)$$

where c_1 and c_2 are the propagation velocities of dilatational and distortional waves in the first medium, whereas c_3 and c_4 are the corresponding velocities in the second one, respectively.

For the case of normal incidence, that is $\alpha_1=0$, all the other angles are zero from Eq. (10);

$$\alpha_1=\alpha_2=\alpha_3=\beta_2=\beta_3=0 \quad \cdots\cdots(11)$$

These relations make A_3 and A_5 to vanish so that dilatational waves generate. The solution for A_2 and A_4 are then given by:

$$A_2=\frac{\rho_b c_3-\rho_a c_1}{\rho_b c_3+\rho_a c_1}A_1 \quad \cdots\cdots(12\,a)$$

$$A_4=\frac{2\rho_a c_1}{\rho_b c_3+\rho_a c_1}A_1 \quad \cdots\cdots(12\,b)$$

(2) Reflected wave

As we see in Eq. (12 a) the amplitude of the reflected wave depends on the values of $\rho_b c_3$ and $\rho_a c_1$, which are the characteristic impedances of the second and first materials, respectively. When the characteristic impedance of the second material, $\rho_b c_3$, is greater than that of the first one, $\rho_a c_1$; namely $\rho_b c_3-\rho_a c_1>0$, the amplitude of the reflected wave has the same sign as that of the incident wave. Since the direction of propagation is reversed on reflection, however, this corresponds to a change in the phase of π in vibration. When the characteristic impedance of the second material is smaller than that of the first, on the other hand, the amplitude of the reflected wave also changes in sign, so that there is no change in the phase on reflection.

Experiments were carried on changing the reac-

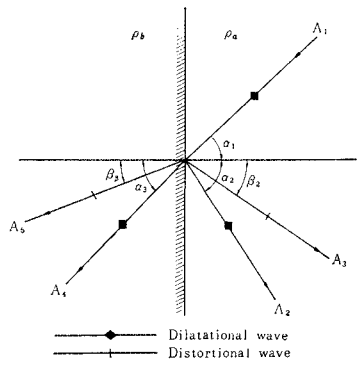

Fig. 13 Reflection and refraction of wave at an interface.

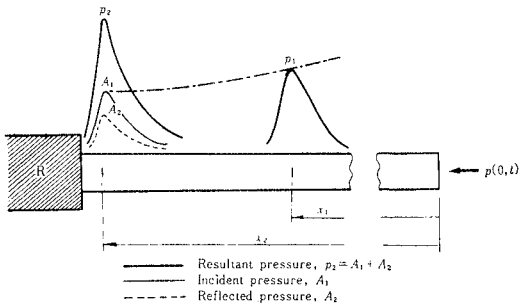

Fig. 14 Resultant of the incident and the reflected waves near the reaction end.

tion end ((R) in Fig. 1) with six kinds of material explained in Table 2. In the experiment the pressures p_1 and p_2 shown in Fig. 14 are measured. Eq. (12 a) gives the relationship between the incident and the reflected waves in terms of displacement amplitudes. These both waves propagate in the same material so that the displacement amplitude can be transformed into the pressure amplitude and, therefore, it should be noted that Eq. (12 a) gives also the relationship between the incident and the reflected waves in terms of pressure amplitudes.

The pressure at the nearest point to the reaction end, p_2, might be regarded as the sum of the incident pressure, A_1, and the reflected one, A_2, then

$$p_2=A_1+A_2 \cdots\cdots(13)$$

The incident wave to the interface, A_1, equals to the pressure attenuating during the distance x_2-x_1, so that it is given from Eq. (4) by

$$A_1=\frac{1}{x_2-x_1}\frac{dx}{dt}\int_{t_1}^{t_2}p_1(t)dt \cdots\cdots(14)$$

Here, $p_1(t)$ is given using the applied surface pressure, $p(0, t)$,

$$p_1(t)=\frac{1}{x_1}\frac{dx}{dt}\int_0^{t_1}p(0, t)dt \cdots\cdots(15)$$

By substituting p_1 measured in the experiment into Eq. (14), the incident pressure amplitude, A_1, is obtained, and by using p_2 measured in the experiment we calculate $p_2/A_1=(A_1+A_2)/A_1$.

On the other hand, the next correlation is obtained from Eq. (12 a), theoretically;

$$\frac{A_1+A_2}{A_1}=1+\frac{\rho_b c_3-\rho_a c_1}{\rho_b c_3+\rho_a c_1}=\frac{2\rho_b c_3}{\rho_b c_3+\rho_a c_1} \cdots\cdots(16)$$

The comparison of the experimental results with the calculated one for each end is illustrated in Fig. 15. In this figure it is very clear that the resultant pressure generated near the reaction end increases with the increase in the rigidity of the end. Thus we can easily call in our mind that a fairly high pressure will be generated in the ground just under the foundation of structure.

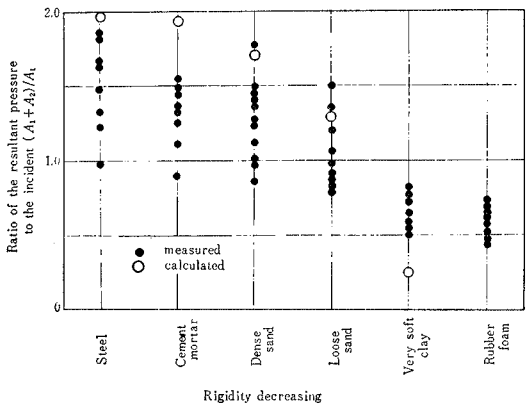

Fig. 15 Resultant stress generated near the various reaction ends.

(3) Refracted wave

The description in **4.** (1) dealing with the reflection of the wave at the interface of two different materials is regarded with the displacement amplitude, and Eqs. (12) relate these waves with each other in terms of the displacement amplitude, A_1, A_2 and A_4. In the case of the reflection of wave, however, the incident and the reflected waves propagate in a same materials, so that Eq. (12 a) can be used in the relationship between the pressure amplitudes in their unchanged form.

That is to say, when σ_1 and σ_2 are to be the pressures of the incident and the reflected waves, respectively, we can use Eq. (12 a) in relating these two pressures by alternating the symbols A_1 and A_2 with σ_1 and σ_2, then

$$\sigma_2=\frac{\rho_b c_3-\rho_a c_1}{\rho_b c_3+\rho_a c_1}\sigma_1 \cdots\cdots(17)$$

Referring to Fig. 16, we assume that the pressure, σ_3, which penetrates into the second material equals to the residual of the incident pressure, σ_1, excluded the reflected pressure, σ_2. By this assumption we get

$$\sigma_3=\sigma_1-\sigma_2=\left(1-\frac{\rho_b c_3-\rho_a c_1}{\rho_b c_3+\rho_a c_1}\right)\sigma_1=\frac{2\rho_a c_1}{\rho_b c_3+\rho_a c_1}\sigma_1 \cdots\cdots(18)$$

This equation is just identical to Eq. (12 b) which shows the relationship between the incident and the refracted waves in terms of the displacement amplitudes.

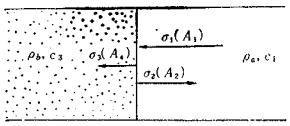

Fig. 16 Reflection and penetration of compressive stress.

In the experiment the second material was prepared as follows. Fine sandy soil passed through a sieve of 0.4 mm was compacted in a cylindrical tube at moderate moisture content. Fig. 17 shows the tube made of alternate rings of vinyl-chloride and rubber, and is about 5.7 cm in diameter. The rings provide necessary radial confinement while the rubber spacers make the tube very soft in the axial

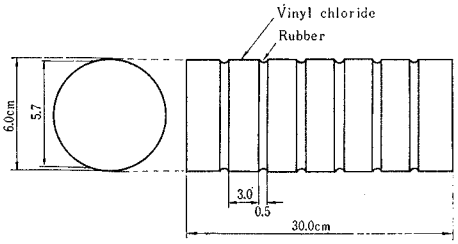

Fig. 17 Cylindrical tube.

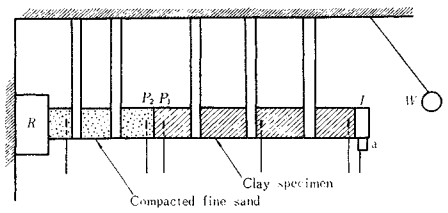

Fig. 18 Experimental apparatus for wave penetration test.

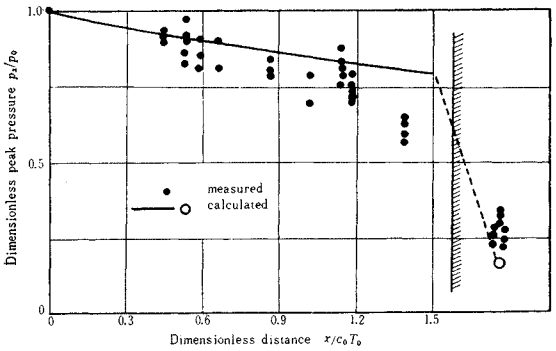

Fig. 19 Wave penetration through two-layered soil column.

direction.

The column compacted with fine sand in it was hunged from the frame and connected with the clay specimen as shown in Fig. 18, and then the impact test was carried on. In order to measure the pressure of the reflected and the refracted (or the penetrated) waves to the dilatational wave incidence, two pressure gauges, P_1 and P_2 in Fig. 18, were embedded at the adjacent points of the interface.

The comparison of the experimental results with the calculated one by Eq. (18) is shown in Fig. 19. Errors in agreement are considered to be because of the rough contact between the clay specimen and the sand column.

5. Conclusion

Throughout the above investigations described in this paper, some interesting and important conclusions can be obtained and are summarized as follows :

(1) The pressure wave attenuates exponentially its peak intensity with distance. The rate of this pressure attenuation is so rapid for soft soil and also when the applied pulsating wave is steep.

(2) The rise time of pressure wave increases with distance and the rate of this increase is large for higher intensity of the pressure peak.

(3) The duration time of pressure wave increases with distance and the rate of this increase is large for soft soil.

(4) The resultant pressure generated near the reaction end increases with its rigidity.

(5) Refracted wave penetrated into the second material measured in the experiment coincides fairly well with the calculated one.

References

1) Salvadori, M.G., R. Skalak and P. Weidlinger : Waves and Shocks in Locking and Dissipative Media, J. ASCE, Vol. 86, No. EM 2, 1960, pp. 77-105.
2) Skalak, R. and P. Weidlinger : Attenuation of Stress Waves in Bi-Linear Materials, J. ASCE, Vol. 87, No. EM 3, 1961, pp. 1-12.
3) Weidlinger, P. and A.T. Matthews : Shock and Reflection in a Non-Linear Medium, J. ASCE, Vol. 91, No. EM 3, 1965, pp. 147-168.
4) Heierli, W. : Inelastic Wave Propagation in Soil Columns, J. ASCE, Vol. 88, No. SM 6, 1962, pp. 33-63.
5) Seaman, L. : One-Dimensional Stress Wave Propagation in Soils, Stanford Research Inst., AD-632106 (DASA 1757), 1966, pp. 1-163.
6) Lawrence, Jr., F.V. : The Response of Soils to Dynamic Loadings, USAEWS, Rep. AD-411210, 1963, pp. 2-8.
7) Seaman, L. : Propagation of Dynamic Stresses in Soil, Proc. Symp. Soil-Structure Interaction, 1964, pp. 98-104.
8) Newmark, N.M. : The Basis of Current Criteria for the Design of Underground Protective Construction, Proc. Symp. Soil-Structure Interaction, 1964, pp. 1-24.
9) Kolsky, H. : Stress Waves in Solids, Dover Publ., N.Y., 1963, pp. 31-34.

(*Received July* 15, 1968)

PARTNER K12

パートナー エンジンカッター

切る

■ 誰でも切れる
スターターを引張るだけで誰にでも簡単にエンジンがかけられます。切断作業は一人で行い、特別の熟練を要しません。

■ どこでも切れる
小型で軽量ですから持ち運びに至便です。その割に馬力は強く、どの様な姿勢でも操作出来、どこでも切れます。

■ 何でも切れる
鉄　　ンクリート、その他何でも　れます。ヒューム管、土管、鉄管、鉄筋など土木建設、その他種々の業務の切断作業に威力を発揮します。

■ はやく切れる
例えばコンクリート道路で3cmの深さ、15mの長さに要する切断時間はわずか約15分です。

■ きれいに切れる
切口はきれいに切れます。切断作業の後バリトリとか仕上とかの必要はほとんどありません。

■ 安全に切れる
特にパートナーカッター用に製作したディスクを用いておりますので切断作業は極めて安全且、迅速に行えます。

日本アレン機械部

東京都豊島区巣鴨7丁目1875番地　TEL(944) 1711(代)
本　　社　東京都千代田区内神田2丁目4-4　TEL(256) 6551(代)
大阪支店　大阪市北区牛丸町55東洋ビル内　TEL(372) 4571(代)
福岡営業所　福岡市薬院町149　TEL 53) 1515
広島営業所　広島市三川町10－13　TEL広島(47) 6351
北海道出張所　北海道苫小牧市音羽町13の11　TEL(苫小牧)2-5016

昭和三十七年五月二十八日第三種郵便物認可
昭和四十四年一月十五日印刷（毎月一回）
昭和四十四年一月二十日発行（二十日発行）

土木学会論文報告集 第161号

価二〇〇〇円